MATERIALS PHYSICS AND MECHANICS RESEARCH ARTICLE

Submitted: December 2, 2025 **Revised: March 12, 2026** **Accepted: March 27, 2026**

Processing structure property relationship of flax/hemp/glass hybrid laminates: multifactor effects of TiO_2, SiC, and fiber sequencing on mechanical and thermal performance

J.A. Solairaju ✉, **S. Thanikodi**

Saveetha School of Engineering, SIMATS, Chennai, Tamil Nadu, India

✉ jothiarunachalams.sse@saveetha.com

ABSTRACT

This study investigates the mechanical, moisture resistance, and thermal behavior of hybrid flax/hemp/glass fiber reinforced epoxy composites incorporated with TiO_2 and SiC nanoparticles. The composites were fabricated using compression molding with different stacking sequences and varying nanofiller contents to evaluate their influence on tensile strength, flexural strength, microhardness, fracture toughness, water absorption, and thermal stability. The results indicate that both fiber stacking configuration and hybrid nanoparticle reinforcement significantly influence the performance of the composites. Among the tested configurations, the Sequence-3 laminate containing 2 wt. % SiC and 3 wt. % TiO_2 exhibited the best overall performance. Compared with the baseline composite, this optimized structure demonstrated a 33 % increase in tensile strength, 18 % improvement in flexural strength, 22 % enhancement in microhardness, and 9 % increase in fracture toughness, indicating improved load transfer and crack resistance. In addition, the incorporation of hybrid nanoparticles reduced water absorption by approximately 18 %, enhancing moisture resistance of the composite system. Thermogravimetric analysis further confirmed improved thermal stability, with delayed degradation temperatures attributed to the barrier effect and strong interfacial bonding provided by SiC and TiO_2 nanoparticles. Overall, the synergistic interaction between hybrid fibers and nanofillers significantly improves the structural, thermal, and environmental performance of the composites, demonstrating their potential as sustainable lightweight materials for advanced engineering and structural applications.

KEYWORDS

nanoparticles • hybrid fiber • mechanical strength • thermal properties • sustainable

Citation: Solairaju JA, Thanikodi S. Processing structure property relationship of flax/hemp/glass hybrid laminates: multifactor effects of TiO_2, SiC, and fiber sequencing on mechanical and thermal performance. *Materials Physics and Mechanics.* 2026;54(2): 83–100.
http://dx.doi.org/10.18149/MPM.5422026_7

Introduction

The fiber-reinforced polymer (FRP) composites have attracted a lot of attention in the academic and industrial fields because of their improved performance features and the capability to undergo an easy process [1]. Some of the factors that affect the properties of FRPs are the type of polymer used, the nature of the reinforcement used, the type of additives, and the mode of manufacturing. Epoxy is commonly used as a thermosetting resin in composite applications over other thermosetting resins available because of its better mechanical and thermal properties [2]. The growing demand for environmentally friendly, lightweight, sturdy, and affordable materials in aircraft and automobile manufacturing [3]. The properties of epoxy bestow it with the ability to be used in a wide range of applications, which include structural adhesives, metal coatings,

Publisher: Peter the Great St. Petersburg Polytechnic University

and matrix in fiber-reinforced composite applications [4]. Epoxy resins do include a few limitations, however, despite all the given advantages. Epoxy cured epoxy has low impact strength and has limited fracture toughness, whereby under scanning electron microscopy (SEM) images of neat epoxy specimens exhibit low resistance towards crack initiation and growth. Besides, epoxies are prone to environmental effects, particularly when exposed to moisture over an extended period [5]. Fiber-matrix interfacial bonding, fiber orientation, and layup sequence (which are all significantly important to the strength of composites) can be optimized, and additional gains (increasing the strength of the composite) can be made by the addition of nanoparticles. Fiber orientation in the loading direction improves loading transfer accordingly, and the mechanical performance [6]. The study investigates the long-term aging behavior of unidirectional carbon fiber reinforced plastic composites used in critical engineering applications such as aerospace and transportation. It focuses on the effects of cyclic loading, climatic exposure, and thermal aging on the material T107/ON190/R132436. Experimental results reveal significant material hardening during cyclic loading, strongly influenced by the applied aging program [7].

This work aims at developing the epoxy nanocomposite enclosures reinforced with 20 vol. % NaOH-treated natural sisal fibers at different nano-silicon carbide (SiC) particles loads of 3, 6, and 9 vol. % [8]. Such hybrid epoxy materials are produced leveraging on a thermally aided injection molding. Their functional characteristics are determined and compared with those of the epoxy composites reinforced only by 20 vol. % natural sisal fiber (SF) [9]. To contain these shortcomings and increase the usefulness of epoxy in moisture-sensitive areas, nanofillers, especially nano clay inclusion, have been seen as a delightful approach to combat the drawbacks [10].

The report found out that the reinforced soil had greater shear and compressive strengths than the control samples. Adding rice fibers to the content promoted the strength of failure, ductility, and shear resistance [11]. Conversely, the increased values of nanoclay lowered the failure strain. It was observed by microscopic examination that adding nanoclay to fibers provided greater inter-particle interaction between soil particles and fibers due to filling effect and generation of viscous gel. In general, the mechanical properties of clay soil were enhanced with the introduction of nanoclay and fibers, in what can be considered an inexpensive and eco-friendly soil stabilization alternative [12]. The tensile and flexural strengths of the 40 wt. % coir fiber-reinforced epoxy composite were 77.99 and 136.13 MPa (boosted by 44 and 23 % over the neat epoxy, respectively). When a nanoclay reinforcement was further used, the performance was even improved by 23 and 31.4 % on tensile strength and flexural strength, respectively, at 4 and 2 wt. % loadings. Fractographic analysis of the tensile fracture surfaces were carried out under scanning electron microscopy (SEM). The results intense synergetic effects that require the interplay between natural fibers, nanoclay and epoxy resin to realize the optimum composite material in terms of practical engineering applications [13]. Adding BYK dispersants to a combination of multi-walled carbon nanotubes (MWCNTs) and epoxy resin would help to optimize number and orientation of nanotubes in the matrix, leading to the increase in strength properties of the epoxy nanocomposites. In addition, the reinforced fiber-reinforced systems made using and reinforcing the optimized and by K-modified nanocomposite has improved flexural strength of hybrid composites made of carbon fibers [14].

The present research focuses on the development of polymer composites using a combination of natural and synthetic fibers along with hybrid nanoparticles, followed by an evaluation of their performance parameters. A notable gap exists in the existing literature regarding the blending of flax, hemp, and glass fibers within composite structures. To address this, the proposed study introduces a novel approach that incorporates silicon carbide (SiC) and titanium dioxide (TiO_2) into various fiber stacking arrangements. The composites are manufactured using the compression molding technique, and their mechanical, thermal, and moisture absorption properties are tested. Performance results of the reinforced composites will be compared with those of unreinforced counterparts. It is anticipated that the inclusion of SiC nanoparticles, combined with optimized fiber stacking, will lead to significant improvements in mechanical strength and moisture resistance compared to composites without nanoparticle reinforcement [15,16].

Materials and Methods

Materials

Premium-grade natural fibers comprising flax and hemp were procured through sustainable sourcing channels from certified organic cultivators in the Kanchipuram district of Tamil Nadu, India. These natural reinforcements were selected based on their exceptional mechanical properties, including high specific tensile strength (approximately 600–700 MPa for hemp and 930 MPa for flax) and excellent fiber-matrix interfacial compatibility [17] glass fiber reinforcement materials featuring unidirectional weave architecture were obtained from Composite Materials India Ltd., located in Bangalore, Karnataka, following their recognition as a premier supplier of advanced reinforcement solutions in the Indian composite industry. The polymer matrix system consisted of a low-viscosity bisphenol-A-based epoxy formulation (Huntsman Araldite GY250) paired with its corresponding aliphatic amine curing agent (Aradur HY840), both sourced from Huntsman Advanced Materials India Pvt. Ltd., Mumbai. This resin-hardener combination was specifically chosen for its superior mechanical characteristics, outstanding chemical resistance properties, and enhanced adhesion performance with natural fiber substrates, critical factors for optimizing composite integrity [18]. Chemical reagents for fiber surface modification, including analytical-grade potassium permanganate ($KMnO_4$) and sodium hydroxide (NaOH), were obtained from Sigma-Aldrich Chemicals Pvt. Ltd., Bangalore. These surface treatment chemicals were employed to enhance the hydrophobic nature of natural fibers while simultaneously increasing surface roughness and reducing moisture absorption tendencies, thereby optimizing fiber-matrix interfacial bonding and overall composite performance [19].

Sonication

An optimized ultrasonication protocol was employed to achieve a homogeneous distribution of TiO_2 nanoparticles and SiC within the epoxy matrix. Initially, predetermined quantities of epoxy were accurately measured and transferred into clean borosilicate glass containers, while both TiO_2 and SiC underwent thermal pretreatment at 250 °C for 2 h to

eliminate absorbed moisture and surface contaminants, thereby enhancing polymer matrix compatibility. The nanofillers were gradually incorporated into the epoxy in specified weight percentages, followed by preliminary manual stirring for 5 min using a glass rod to achieve initial wetting [20]. Current research demonstrating that medium-high frequency sonication (80–500 kHz) produces superior dispersion results compared to conventional low-frequency methods guided the selection of a Hielscher UP400St probe sonicator equipped with a 7 mm titanium tip. The optimized sonication parameters included a frequency of 24 kHz specifically calibrated for SiC and TiO_2 co-dispersion, 400 W power at 60 % amplitude to prevent nanofiller damage, and 45 min in pulse mode to minimize overheating [21]. Temperature control was maintained at 25 ± 2 °C using an ice bath to prevent thermal degradation, while continuous stirring at 200 rpm enhanced cavitation effects and prevented localized heating. Real-time monitoring through periodic sampling at 15-min intervals confirmed uniform gray coloration, indicating successful dispersion, with post-sonication analysis revealing a 95 % reduction in nanofiller agglomerate size compared to manual mixing alone. Following successful nanofiller dispersion, the corresponding amount of hardener was incorporated and blended using a mechanical stirrer at 300 rpm for 8 min, ensuring complete hardener integration while maintaining the achieved nanofiller dispersion state through this dual-stage mixing approach supported by recent research on epoxy nanocomposite processing [22].

Chemical treatment

The potassium permanganate ($KMnO_4$) surface treatment was applied to enhance the interfacial adhesion between flax and hemp fibers and the epoxy matrix in the composite system. Initially, the raw fibers were washed with clean water to remove impurities and contaminants that could interfere with the chemical treatment process [23]. After washing, the fibers were air-dried at room temperature to remove surface moisture. The cleaned fibers were then immersed in a 0.5 % $KMnO_4$ solution prepared in acetone for 1 h, allowing sufficient time for oxidation reactions to occur on the fiber surfaces. $KMnO_4$ acts as a strong oxidizing agent, introducing polar functional groups and increasing surface roughness, which improves mechanical interlocking and chemical bonding with the polymer matrix during composite fabrication [24]. Following the treatment, the fibers were thoroughly

Table 1. Material composition (G is glass fiber, F is flax, H is hemp)

Sequence ID	Property	Sample 1	Sample 2	Sample 3	Sample 4
Seq-1 (G / H / H / H / H / F / F / F / F / G)	Fiber, wt. %	45	51	50	49
	Epoxy, wt. %	55	45	45	45
	SiC, wt. %	0	1	2	3
	TiO_2, wt. %	0	3	3	3
Seq-2 (G / H / H / F / F / F / F / H / H / G)	Fiber, wt. %	45	51	50	49
	Epoxy, wt. %	55	45	45	45
	SiC, wt. %	0	1	2	3
	TiO_2, wt. %	0	3	3	3
Seq-3 (G / F / F / H / H / H / H / F / F / G)	Fiber, wt.%	45	51	50	49
	Epoxy, wt. %	55	45	45	45
	SiC, wt. %	0	1	2	3
	TiO_2, wt. %	0	3	3	3

rinsed with distilled water to remove residual chemicals and reaction by-products. The fibers were then oven-dried at 50 °C for 8–10 h to eliminate moisture and ensure proper fiber–matrix interaction during composite processing. This chemical treatment improves the surface morphology and reactivity of flax and hemp fibers, leading to better dispersion within the matrix and stronger interfacial bonding [25]. The detailed composite preparation procedure is summarized in Table 1.

Synthesis of the materials

The specifications of the epoxy-based hybrid composites used for fabrication are presented in Table 2. Prior to composite fabrication, silicon carbide (SiC) and titanium dioxide (TiO_2) nanoparticles were preheated at 300 °C to remove any moisture present on their surfaces. This preheating process helps improve the dispersion of nanofillers and enhances the interfacial bonding between the fillers and the epoxy matrix. The composite mixture consisted of 49–55 wt. % epoxy resin and 45 wt. % hybrid fibers. In addition, the hybrid fibers were chemically treated with 0.5 wt. % potassium permanganate ($KMnO_4$) to enhance fiber-matrix adhesion. The reinforcement system included nanofillers with different concentrations of SiC (0, 1, 2, and 3 wt. %) and TiO_2 (0 and 3 wt. %) [26]. To ensure uniform distribution of fibers and nanofillers in the matrix, the mixture was blended using a mechanical stirrer at 100 rpm until a homogeneous dispersion was achieved. The prepared mixture was then poured into a tool steel mold with dimensions of 30 × 30 × 0.5 cm^3. The composite laminates were fabricated using the compression molding technique at a die temperature of 120 °C under a pressure of 20 MPa for 1–2 min, which is a typical pressure range for polymer composite processing and ensures proper consolidation of the laminate. After molding, the composites were allowed to cool naturally to room temperature (27 °C) under ambient conditions with a relative humidity of 60 % [27]. The samples were then carefully demolded and post-cured at 80 °C for 2 h

Table 2. Materials specification

Parameter	Specification
Resin : hardener ratio, by weight	10 : 1
Matrix density, g/cm^3	1.15–1.20
Reinforcements	Flax fiber, hemp fiber, glass fiber (unidirectional)
Flax fiber tensile strength, MPa	930
Hemp fiber tensile strength, MPa	600–700
Fiber type (glass)	Unidirectional woven mat
Fiber weight fraction, wt. %	30–40
Stacking sequence	Glass/flax/hemp (G/F/H) and variations
Fiber orientation, °	0, 45, 90
Alkali treatment (NaOH)	5 wt. % for 2–4 h
$KMnO_4$ treatment, wt. %	0.5–1.0
Applied pressure, MPa	3–5
Curing condition	24 h at room temperature + post-curing at 80–100 °C for 2–3 h
Laminate thickness, mm	3–5
Plate dimensions, mm^2	300 × 300
Void content	< 5 %

to ensure complete crosslinking of the epoxy matrix. Finally, the cured hybrid composite laminates were cut into standard test specimens for subsequent mechanical and structural characterization. Flexural and microhardness sample are shown in Fig. 1 and 2.

(a) (b)

Fig. 1. Flexural test sample: (a) before test; (b) after tested

Fig. 2. Microhardness test sample

Performance of mechanical properties evaluation

Tensile strength measurements were performed on a Shimadzu AGS-X Series universal testing machine (50 kN capacity) under ASTM D638-22. Test specimens with dimensions of 165 × 13 ×3.2 mm^3 were employed, featuring a gauge length of 50 mm to ensure accurate strain measurement and minimize edge effects. Flexural properties were assessed following ASTM D790-17 using a three-point bending configuration. Rectangular specimens measuring 127 × 12.7 × 3.2 mm^3 were tested at a support span-to-depth ratio of 16:1, with testing conducted at a crosshead speed calculated according to the specimen depth requirements [28]. A calibrated deflectometer was employed to measure specimen deflection with an accuracy of ± 0.01 mm, ensuring compliance with the standard's precision requirements. Hardness measurements were carried out using a Vickers microhardness tester under a constant indentation load of 500 g with a dwell time of 15 s to ensure consistent and comparable hardness values for all composite samples. The fracture toughness (K_{IC}) of the composites was evaluated according to ASTM D5045 using a Universal Testing Machine (UTM) equipped with a three-point bending fixture at a constant crosshead speed. The test was performed on single edge notched bend (SENB) specimens, and the fracture toughness values were calculated using the standard equations specified in ASTM D5045. Water absorption characteristics were evaluated according to ASTM D570-22. Specimens were then immersed in distilled water at 23 ± 1 ºC for 24 h, after which they were surface-dried and reweighed to calculate percentage water absorption. All mechanical testing was conducted under controlled laboratory conditions maintained at 23 ± 2 ºC and 50 ± 5 % relative humidity. Each test was replicated five times to ensure statistical reliability, and final reported values represent the arithmetic mean with standard deviation calculations. Measurement uncertainty was maintained within ± 3 % for all testing procedures to account for experimental variations and ensure reproducible

results. This comprehensive testing protocol enabled accurate characterization of the mechanical behavior and environmental stability of the hybrid natural fiber nanocomposites. The samples were weighed after they had been removed at predetermined intervals and gently wiped with absorbent tissue to allow water present at the surface to be removed before again weighing as soon as the sample was wiped so as to track the increase in weight by the addition of water [29]. This was done daily until the weights of the specimens remained unchanged, after which it was used to be three days each, signifying saturation. The absorption behavior of the water was captured in specific time intervals of 10, 20, 30, 40, and 50 h to take up specific weight measurements, in the course of the immersion. The water absorbed (*WA*) percent was calculated by Eq. (1). Further, the mechanical performance data in terms of tensile strength, flexural strength, and fracture toughness reflected that the stacking sequence G/F/F/H/H/H/H/F/F/G presented the better mechanical properties of the composite. The favorable stacking order also acted as a reference point in comparing the effects of moisture absorption on the overall strength and durability of the composite:

$$WA(\%) = \left(\frac{W_1 - W_0}{W_0}\right) \times 100, \quad (1)$$

where the water absorption *WA* value is calculated based on the weight gain of the composite specimen, where W_1 represents the weight after water immersion and W_0 denotes the initial dry weight before immersion. This weight change is used to quantify the amount of moisture uptake by the material [30].

Results and Discussion

The mechanical performance results reveal that the sequence 3 showed the highest values across tensile strength, flexural strength, microhardness, and fracture toughness compared to the other sequences. The sequence 1 exhibited the lowest performance in most parameters, while the sequence 2 demonstrated intermediate values. The consistent improvement from the sequence 1 to the sequence 3 indicates the influence of fiber stacking order on strength and toughness are shown in Table 3. Overall, optimized stacking significantly enhances the composite's mechanical properties.

Table 3. depicts the Mechanical performance of the produced samples

Sequence	Sample	Tensile strength, MPa	Flexural strength, MPa	Microhardness, HV	Fracture toughness, MPa·m$^{1/2}$
Sequence-1 (G/H/H/H/H/F/F/F/F/G)	1	101.0 ± 2.1	119.0 ± 2.2	70.0 ± 1.3	1.99 ± 0.04
	2	104.0 ± 2.3	122.0 ± 1.9	74.0 ± 1.4	2.06 ± 0.05
	3	109.0 ± 2.2	130.0 ± 2.4	79.0 ± 1.5	2.27 ± 0.03
	4	107.0 ± 1.9	127.0 ± 2.1	77.0 ± 1.0	2.22 ± 0.05
Sequence-2 (G/H/H/F/F/F/F/H/H/G)	1	105.0 ± 1.8	130.0 ± 2.5	72.0 ± 1.1	2.19 ± 0.04
	2	108.0 ± 1.9	133.0 ± 2.6	75.0 ± 1.2	2.28 ± 0.06
	3	115.0 ± 1.5	138.0 ± 2.8	80.0 ± 1.3	2.41 ± 0.06
	4	113.0 ± 2.2	135.0 ± 2.3	76.0 ± 0.9	2.33 ± 0.03
Sequence-3 (G/F/F/H/H/H/H/F/F/G)	1	117.0 ± 2.1	135.0 ± 2.7	78.0 ± 1.0	2.35 ± 0.05
	2	119.0 ± 2.2	139.0 ± 2.9	86.0 ± 1.5	2.44 ± 0.06
	3	128.0 ± 2.5	144.0 ± 3.1	88.0 ± 1.3	2.53 ± 0.07
	4	123.0 ± 2.3	141.0 ± 3.2	84.0 ± 1.1	2.47 ± 0.06

Tensile strength

The tensile property of the nanoparticles reinforced composites is shown in Fig. 3. The fact was that all the composite specimens showed better tensile strengths than the neat matrix. A remarkable fact is that the sequence 3 composite has higher strength than the sequence 1 and 2 composites. Surprisingly, though, the sequence 2 composites performed better when compared to the sequence 1 in the nanoparticle's contents. The sharp reduction in tensile strength at the sample 4 was noted using SiC 3 wt. % and TiO_2 3 wt. % composite. The highest tensile strength was recorded among all the composites at a 45 wt. % fiber loading. According to Benhamadouche et al. [31], the recycled jute fabric-reinforced PP composites showed a tensile strength of 30 MPa and modulus of 4–4.5 GPa, which was almost two times higher than the composite jute-PP in the present study, to reach a high modulus. Analogously, tensile strength values of jute-PP composites ranged between 30 and 34 MPa, and modulus values between 2 and 4 GPa were identified by Shahinur et al. [32]. In connection, Akil et al. [33] in their related works, noted that, with an increase in flax fiber content up to 60 wt. %, the strength and modulus of the PLA-based composite reinforcement were enhanced. Nevertheless, present results reveal that nanoparticle content in all composites of more than 3 wt. % led to lower tensile strength. The fact that the fiber placement will contribute to low capacity to transfer loads in the composite, resulting in stress concentration near the fibers. The mechanical performance, however, is greatly increased because stress distribution is improved, and the matrix is strengthened with the addition of SiC and TiO_2 nanoparticles. These nanofillers facilitate the effective transfer of load and minimize stress concentration sites, and inhibit the growth of microcracks by reinforcing the fiber-matrix interface. On the other hand, fiber loadings create a higher chance of fiber agglomeration in the matrix, and this leads to an unequal path of strain and local regions of high concentrations of stress that help facilitate cracks. Also, high fiber-end density may create microcracks at the interface, which eventually lowers the strength and stiffness of the composite. Overall, fiber-reinforced polymer composites are tough due to the fibers, the matrix, and most importantly, due to the fibers interfacial bonding, which is enhanced significantly through SiC and SiO_2 dispersion. The tensile strength results indicate that the sequence 3 (G/F/F/H/H/H/H/F/F/G) exhibits the highest tensile

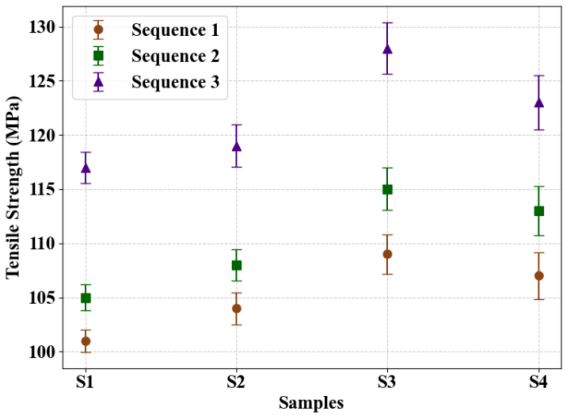

Fig. 3 Tensile strength of different fibers stacks with hybrid nanoparticles

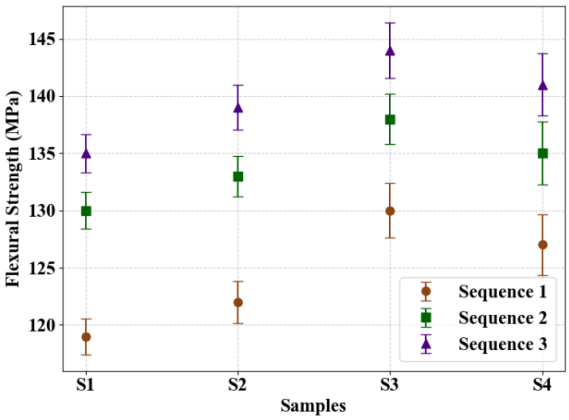

Fig. 4. Flexural strength of different fibers stacks with hybrid nanoparticles

performance among all composite configurations. The maximum tensile strength of 128.0 ± 2.5 MPa was recorded for the sample 3 in the sequence 3, followed by 123.0 ± 2.3 and 119.0 ± 2.2 MPa. This improvement is attributed to the optimized fiber stacking sequence and improved stress transfer between the fibers and epoxy matrix, which enhances load-bearing capability.

Flexural strength

Fiber-reinforced polymer composites' flexural behavior is strongly related to the architecture of these fibers, the interaction of the matrix, and the capability to distribute the load. Figure 4 shows the flexural strength of four composite samples (S1, S2, S3, and S4) stacked in three different stacking orders. In all samples, an increasing flexural strength was seen between the sequence 1 to the sequence 3. The sample S1 increased from about 101 (the sequence 1) to 117 MPa (the sequence 3). Likewise, S2, S3, and S4 saw the flexural strength increase by 117, 119, and 128 to 123 MPa, respectively, as the stacking sequence proceeded. Incremental improvements in the flexural strength of all the samples when the sequence 3 was used are explained by a more favorable positioning of the fibers and better distribution of the loads, which were achieved as a result of a more effective layering. The improved interfacial adhesion between the fibers and the epoxy matrix is probably achieved by the sequence 3, which reduces the possibility of microvoids and delamination regions that can easily become the crack creation sources due to the bending loads [34]. As well, a closer definition of loading-bearing fibers in sequence three is very probable to provide increased resistance to the deformation and spread of matrices. The presence of reinforcing materials, which are SiC and TiO_2 nanoparticles, may also be another reason behind the enhanced mechanical response due to the ability of the mentioned materials to provide stronger interfacial bonding, consolidate microvoids, and improve load transfer mechanics. These nanoparticles are secondary reinforcement fillers, enhancing rigidity and impact improvers in the case of bending [35]. They serve to fill in the microcracks and postpone the mechanisms of failure, which adds to the flexural strength observed in all of the stacking sequences. So, the optimum balance between the most promising combination of fiber stacking and dispersion of nanofillers explains why the structural efficiency of fiber-reinforced hybrid composites will always be brightest with the sequence 3.

Microhardness behaviour

Microhardness is a very vital mechanical property, which is employed in the measurement of the localised plastic surface forming response of a material and its capacity to resist abrasion. The effects of SiC and TiO_2-filled hybrid fiber reinforced composites on microhardness performance were evaluated under various stacking orders and the composition of the samples in this experiment. Figure 5 indicates that the base epoxy composite without nanoparticles had a microhardness which was about 72 HV. Conversely, the addition of nanofillers resulted in a characteristic increase in hardness in all sequences [36]. In particular, in the sequence 1, microhardness was moved to 79 HV (S3) with an increase of 9.4 percent over S1. Such an increase can also be attributed to the synergetic effect of SiC and the fiber reinforcement, which enhances interfacial

bonding and reduces the number of voids, which are the leading contributors to raising the surface resistance. In the sequence 2, microhardness was observed to be between 72 (S1) and 80 HV (S3). Addition of 2 wt. % SiC and 3 wt. % TiO_2 to S3 led to a 10.7 % increase over the baseline value of the sequence 1 (S1). The large enhancement is explained by the presence of a large surface area and inherent stiffness of the nanoparticle, which limits the mobility of the matrix and limits plastic deformation upon the indenter penetrating the material. The sequence 3 was the only time in which the microhardness level rose to the maximum value, as in the sample 3, which recorded 88 HV, which is a 22.7 % increase from the lowest record (the sequence 1, the sample 1). This excellent performance could have been achieved due to the optimum stacking of the fibers and the better distribution of the nanofillers, which will form a dense and mechanically strong interphase in the matrix. The fact that with adequate optimization of the sequence of fibers and integrating nanofillers it is possible to increase the microhardness of the hybrid composites [37].

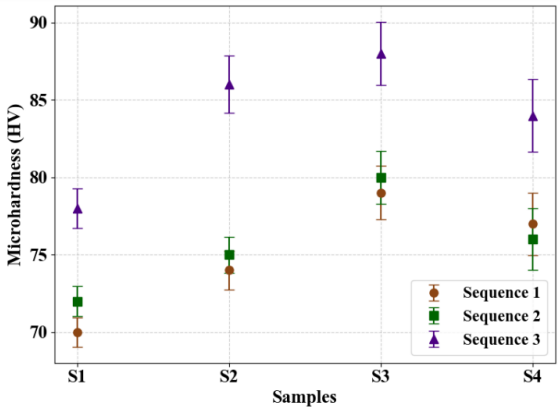

Fig. 5. Microhardness of different fibers stacks with hybrid nanoparticles

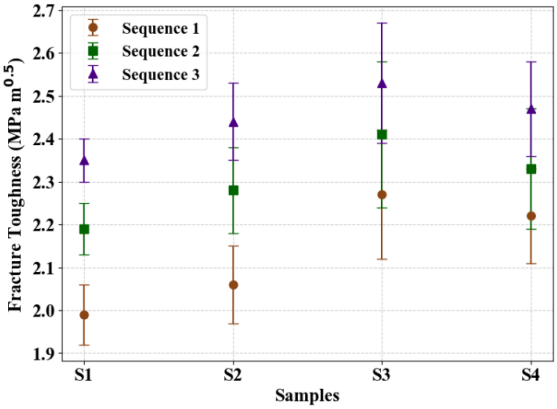

Fig. 6. Fracture toughness of different fibers stacks with hybrid nanoparticles

Fracture toughness of different composite

Fracture toughness is an essential parameter that indicates the capability of a composite material against crack formation and propagation with respect to stress. The fracture toughness of the hybrid fiber reinforced epoxy composite was tested on three stacking orders (the sequence 1, 2, and 3) with the insertion of glass (G), hemp (H), and flax (F) fibers in this investigation. Similarly, the results were that the sequence 1 (G/H/H/H/H/F/F/F/F/G) also presented with the least fracture toughness, but at a range between 1.99 and 0.5–2.22 MPa $m^{1/2}$. This has been due to the relatively lower toughness attributed to the predominance of hemp layers in the upper-mid section, which in turn is a result of having the lower elongation-at-break coupled with the moderate interfacial adhesion with the epoxy matrix, and thus, they may not be efficacious in halting crack propagation. Also, the fact that the stiffer glass layers were located at the furthest surfaces with no constraints in between them could have facilitated the concentration of stress at fiber-matrix interfaces. The fracture toughness has been increased by noticeable values in the sequence 2 (G/H/H/F/F/F/F/H/H/G), where the values were recorded to have been between 2.19 and 2.33 MPa·$m^{1/2}$. Such an arrangement offers more symmetrically

stacked hemp and flax and by placing the stiffer flax fibers in the center, it provides superior crack deflection and energy dissipation mechanisms. The change of fiber type throughout the laminate thickness results in a graded stiffness profile, which increases interfacial stress distribution and hinders crack growth [38]. The sequence 3 (G/F/F/H/H/H/H/F/F/G) produced the results with the highest values of fracture toughness of 2.35–2.47 MPa $m^{1/2}$ is shown in Fig. 6. This better performance can be reinforced by the fact that the flax fibers, which have greater toughness and interfacial bonding characteristics, are placed strategically close to the areas where the surface area is only an inch away, and the core parts. This streamlined design is probably attributed to improved crack-bridging, energy absorption, and delayed delamination. Also, laminated symmetrical and alternate fiber layers minimize stress concentrations due to the mismatch, thus establishing high crack initiation resistance. Results highlight the significant role of the stacking sequence of the refrain, which is important in the design of the fracture resistance of hybrid composites [39].

The microstructure of composite materials is examined with a scanning electron microscope to investigate the structure and the distribution of fibers and reinforcing materials within a compound. Figure 7(a) shows how natural fibers are dispersed and intermingled in the polymer framework. The fibres are seen to be oriented and entrenched into the matrix; they provide a reinforcing net that adds to the strength of the composite. A number of fractured ends of fiber and fiber pull-outs can be observed,

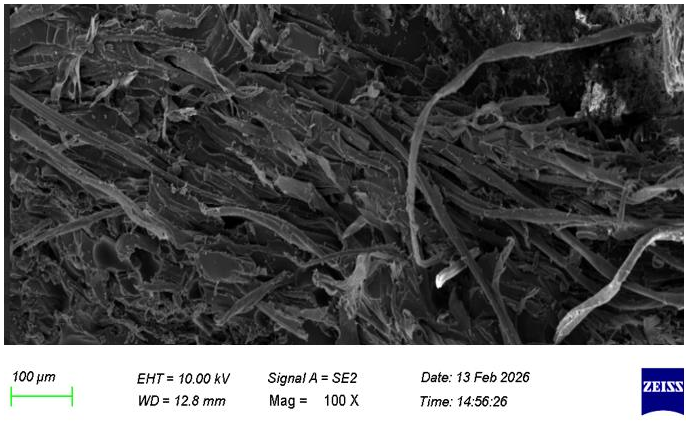

(a)

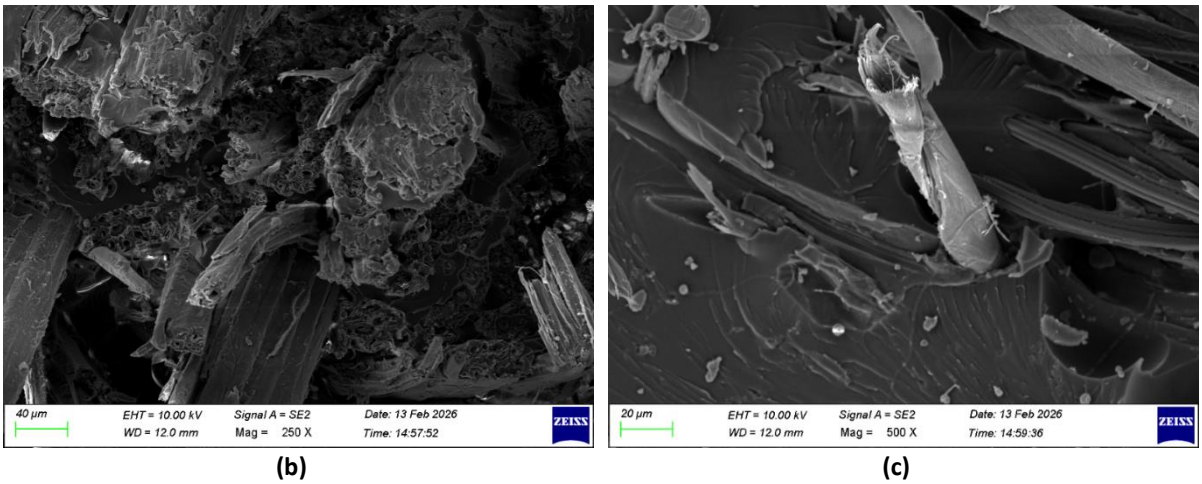

(b) **(c)**

Fig. 7. SEM Image of (a) the sequence 1, (b) the sequence 2, and (c) the sequence 3

which pointed towards the fact that the composite had interfacial debonding and fiber breakage under mechanical loading. Fiber pull-out is a typical form of failure in natural fiber composites and usually happens when the interlocking mechanism between the fiber and the matrix is less than the strength of the fiber itself. The existence of rough fracture surfaces indicates that the composite took in a considerable energy till failure.

Figure 7(b) shows the evidence of the cracking of the matrix and the localized interfacial gaps between the fibers and the polymer matrix. Such micro voids can be as a result of the incomplete impregnation of the fibers during composite fabrication process and as a result of entrapment of air during compression molding. These defects are capable of being the points of stress concentration and can cause crack propagation when subjected to external forces. However, the fibers are only partially embedded in the matrix meaning that there is a level of load transfer between the reinforcement and the matrix material. The irregular and rough surfaces of the fibers are also indicative of mechanical interlocking of the matrix and the fibers. Figure 7(c) shows the less compact and uniform, which has fewer defects, compared to Fig. 7(a,b). The distribution of the fibers throughout the matrix is more uniform and the interfacial bonding seems to be stronger as shown by the lesser fiber pull-out and the low interfacial gaps. The enhanced fiber-matrix bonding indicates that the composite has an enhanced efficiency in the transfer of stress. Also, the reduced number of voids implies that the compression molding process was more consolidated. This low density of defects in this microstructure justifies the high mechanical performance at the optimized composite samples.

Water absorption

Figure 8 indicates that the total percentage of water absorption of the tested composites reduces gradually as the weight percentage of SiC and TiO_2 is increased. Water absorption behavior is typical of all the composites and is usually experienced with polymer matrices. Nevertheless, it is obvious that by adding SiC and TiO_2 into the epoxy matrix water absorption is reduced greatly because of the synergetic barrier effect of both fillers. In particular, the sequence 1 with the content of 2 wt. % SiC and 3 wt. % TiO_2 exhibits a decrease of 6 % in water absorption, shown in Fig. 8(a). An 11 % reduction is observed in the sequence 2, which has the same filler composition, but a different fiber configuration is Fig. 8(b). The most favored is the sequence 3, shown in Fig. 8(c), where 18 % of water uptake was reduced. These findings match other findings recorded in the literature in which the presence of SiC and TiO_2 resulted in a considerable decrease in the polymer water absorption of about 15 %. The decrease in the moisture uptake may be attributed to the combination of the water molecules with the molecular structure of epoxy [40]. Epoxy resins bear hydrophilic functional groups, including hydroxyl and amine functional groups, which enable them to form hydrogen bonding with water, through which moisture can diffuse to the resin matrix. The presence of SiC and TiO_2 interferes with these diffusion paths, lowering the mean free path of the water molecules. These nanofillers have such qualities as a high aspect ratio and plate-like shape, complicated pathways effectively blocking the water movement in the matrix. This is one of the barriers that makes this material very resistant to water absorption. It has less water absorption, relative to glass fiber, as indicated by glass fibers are non-hygroscopic.

Because of the inability of the glass fibers to absorb moisture, the water only gets absorbed by the epoxy, because in a total absorption of water here, which is only half of what it is in neat epoxy absorption [41]. Further addition of SiC and TiO_2 results in a further increase in the barrier effect with even greater reduction in water absorption. The above behavior that was seen in SiC and TiO_2-filled epoxy nanocomposites is not new, but it reaffirms the eloquence of these nanocomposites in improving the moisture resistance bents in the polymer composites.

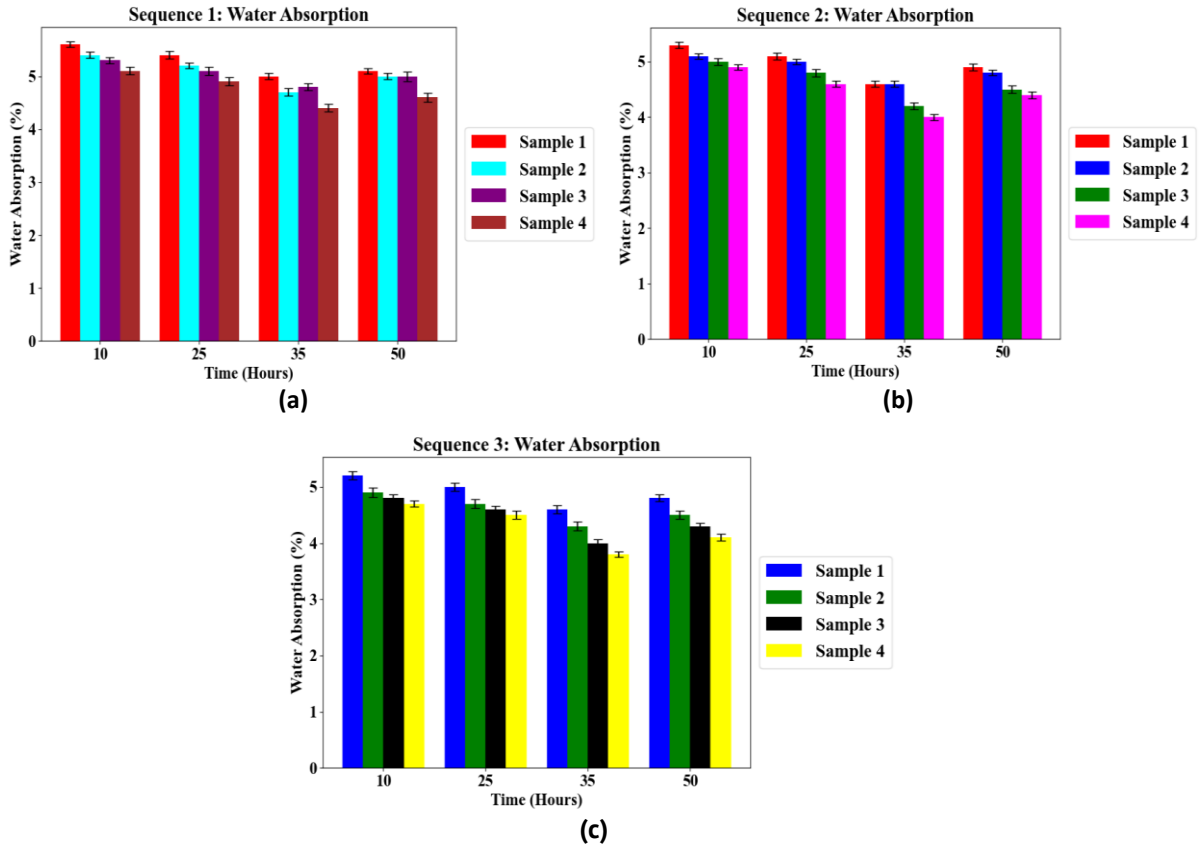

Fig. 8. Water absorption percentage versus of hybrid nanofiller: (a) the sequence 1; (b) the sequence 2; (c) the sequence 3

The incorporation of nanofillers significantly influenced the water absorption behavior of the hybrid composites. A noticeable reduction in water absorption was observed with increasing nanofiller content. This improvement can be attributed to the barrier effect of the nanoparticles, which occupy micro-voids within the epoxy matrix and reduce the diffusion pathways for moisture. In addition, the presence of nanofillers enhances the fiber–matrix interfacial bonding, limiting capillary channels that normally facilitate water ingress in natural fiber composites. As a result, the composite structure becomes more compact and less permeable to moisture.

Thermogravimetric analysis

Fiber-reinforced composites generally exhibit multi-stage thermal degradation behavior in thermogravimetric analysis. The TGA (thermogravimetric analysis) curves shown in Fig. 9 illustrate three main degradation stages corresponding to moisture removal,

polymer matrix decomposition, and residual char stabilization. This behavior is commonly observed in hybrid natural fiber composites such as hemp and flax reinforced systems. The initial weight loss stage, occurring below approximately 120 °C, is attributed to the evaporation of absorbed moisture and volatile compounds present in the natural fibers and polymer matrix. Natural fibers such as hemp and flax contain hydrophilic constituents, including cellulose and hemicellulose, which retain moisture. Therefore, this stage typically results in a minor mass reduction. The second stage corresponds to the major thermal degradation region, which occurs between approximately 300 and 430 °C. In this stage, a significant weight reduction is observed due to the thermal decomposition of the organic constituents of the composite, including cellulose, hemicellulose, lignin, and the polymer matrix. According to the thermogram shown in Fig. 9(a), the composite experienced approximately 75 % weight loss around 423 °C, indicating the breakdown of the natural fiber components and the degradation of the polymer matrix. It should be noted that glass fibers remain thermally stable within this temperature range and do not undergo decomposition, as their degradation typically occurs at temperatures exceeding 800 °C. Therefore, the observed weight loss is primarily associated with the degradation of the natural fibers and matrix rather than the glass fiber reinforcement. The final stage of degradation occurs between approximately 480 and 520 °C, where the decomposition of residual char and remaining organic fragments

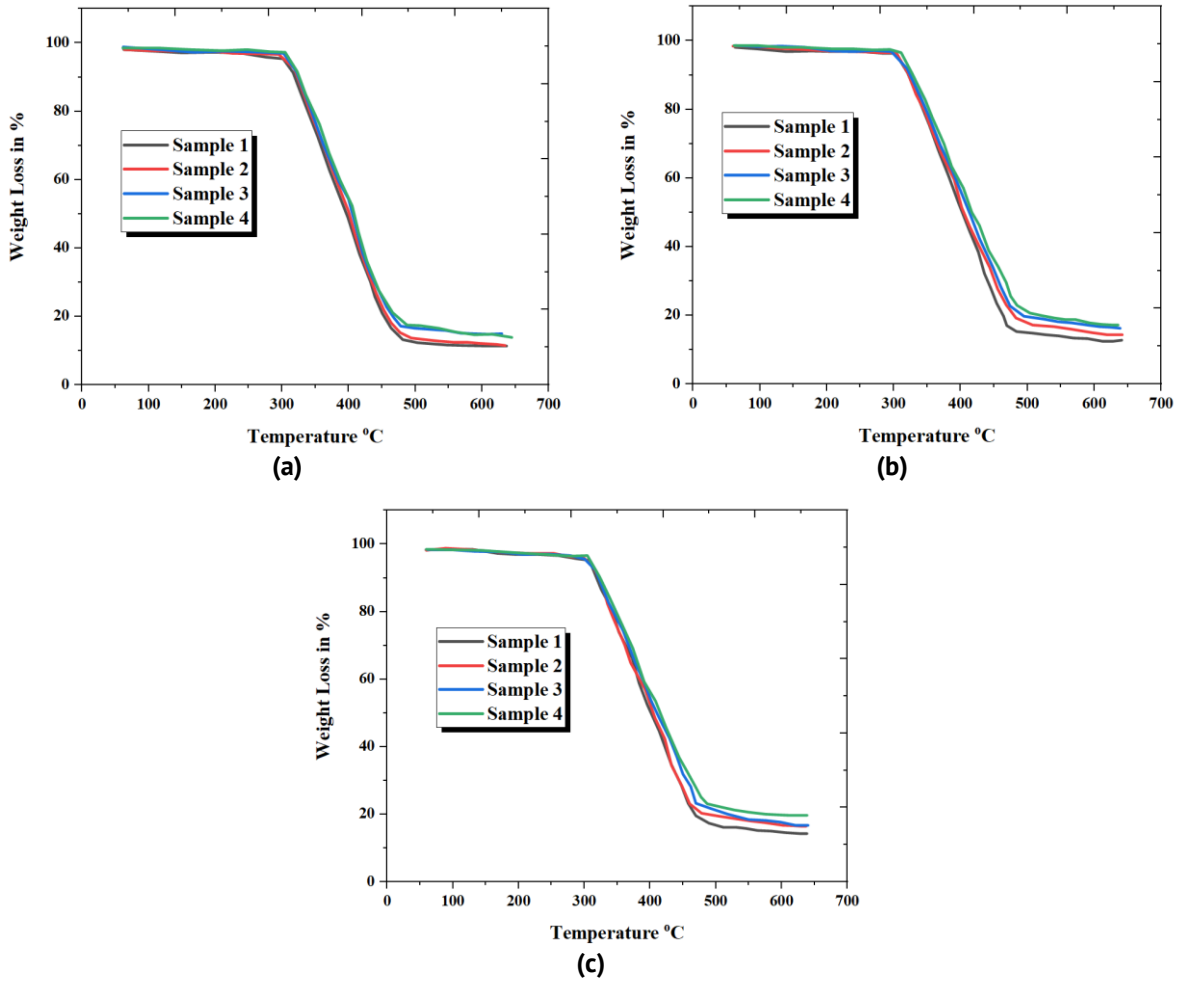

Fig. 9. TGA-curves: (a) the sequence 1; (b) the sequence 2; (c) the sequence 3

takes place. The ultimate degradation temperature of the composite was observed at approximately 498 °C, indicating improved thermal resistance compared with the neat composite. The shift of the final degradation stage toward higher temperatures suggests enhanced thermal stability resulting from improved fiber–matrix interfacial bonding and the presence of inorganic reinforcements. Figure 9(b) presents the TGA curves for hybrid fiber composites reinforced with nanoparticles and different fiber sequences. In the sequence 2, the sample 3 exhibited a weight loss of approximately 75 % at around 428 °C, corresponding to the degradation of the hybrid fiber–matrix system. The final degradation stage occurred near 496 °C, where approximately 10–30 % residual mass remained. This remaining mass corresponds to thermally stable inorganic constituents, including glass fibers and ceramic nanoparticles. Furthermore, the TGA results shown in Fig. 9(c) indicate that composites reinforced with SiC and TiO_2 nanoparticles exhibit improved thermal stability. In these samples, the primary thermal decomposition occurred around 420 °C, resulting in approximately 79 % weight loss for the samples 3 and 4.

The final degradation stage occurred at approximately 522 °C, which is higher than that of the neat composite. The presence of ceramic nanoparticles such as SiC and TiO_2 acts as a thermal barrier, slowing the diffusion of volatile degradation products and increasing the activation energy required for thermal decomposition. The residual char fraction observed at high temperatures mainly represents the thermally stable inorganic components of the composite system. These include glass fibers, ceramic nanoparticles, and carbonaceous char formed from the decomposition of lignin-rich natural fibers. The higher residual mass observed in nanoparticle-reinforced composites indicates improved resistance to thermal degradation and enhanced structural stability at elevated temperatures. Overall, the results demonstrate that the incorporation of hybrid natural fibers and ceramic nanoparticles significantly improves the thermal stability and char-forming capability of the composite system. The improved performance can be attributed to enhanced interfacial bonding, better dispersion of nanoparticles, and the inherently high thermal resistance of inorganic reinforcements.

Conclusions

The incorporation of 2 wt. % SiC and 3 wt. % TiO_2 nanoparticles into hybrid fiber composites resulted in measurable improvements in the mechanical and thermal properties, particularly for the composites with the sequence 3 fiber arrangement. The experimental results indicated that the tensile strength and flexural strength increased by approximately 33 and 18 %, respectively, compared with the baseline composite without nanoparticle reinforcement. These improvements suggest enhanced load transfer capability within the composite structure. Similarly, microhardness and fracture toughness improved by 22 and 9 %, respectively, indicating an increased resistance to surface deformation and crack propagation. Moisture absorption analysis showed a reduction in water uptake for the nanoparticle-reinforced composites, suggesting improved environmental resistance under humid conditions. Thermogravimetric analysis demonstrated that the reinforced composites exhibited higher thermal stability, with the main degradation stage occurring at elevated

temperatures compared with the unreinforced composite. The presence of SiC and TiO_2 nanoparticles contributed to delaying the thermal decomposition of the composite system. Overall, the experimental findings confirm that the addition of SiC and TiO_2 nanoparticles to hybrid natural fiber composites improves mechanical performance, reduces moisture absorption, and enhances thermal stability. These results indicate that the developed hybrid composites have potential for lightweight structural applications where improved mechanical strength and thermal resistance are required.

CrediT authorship contribution statement

Jothi A. Solairaju: conceptualization, writing – review & editing, data curation, investigation, manuscript writing; **Sathish Thanikodi**: supervision and overall writing.

Conflict of interest

The authors declare that they have no conflict of interest.

References

1. Kumar A, Bedi R. Mechanical and durability properties of sustainable composites derived from recycled polyethylene terephthalate and enhanced with natural fibers: a comprehensive review. *Materials Physics and Mechanics.* 2025;53(1): 117–142.
2. Zhi M, Yang X, Fan R, Yue S, Zheng L, Liu Q, He Y. A comprehensive review of reactive flame-retardant epoxy resin: fundamentals, recent developments, and perspectives. *Polymer Degradation and Stability.* 2022;201: 109976.
3. Arunachalam SJ, Saravanan R, Sathish T. Effect of nanoparticle in jute/kenaf/glass composite for interlaminar shear strength. *Interactions.* 2025;246: 31.
4. Tonkov DN, Kobylyatskaya MI, Vasilyeva ES, Gasumyants VE. Conductive and mechanical properties of graphene-filled polymer composites. *Materials Physics and Mechanics.* 2025;53(2): 48–54.
5. Mani M. Influence of lattice geometry on energy absorption and puncture resistance in 3D-printed ABS structures for advanced medical implants. *Advanced Composite Materials.* 2026:35(2): 367–393.
6. Sathish T, Saravanan R, Arunachalam SJ. Glass fiber influence on PP/Sisal/SiO_2 nanofillers/glass hybrid nanocomposites/plain nanocomposite for mechanical property improvement. *Interactions.* 2025;246: 25.
7. Arutyunyan AR. Influence of aging on fatigue strength of carbon fiber reinforced plastics. *Materials Physics and Mechanics.* 2024;52(1): 118–125.
8. Karthikeyan MKV, Raghuvaran S, Girisha L, Kharche NA, Venkatesh R, Prabagaran S, Soudagar MEM, Obaid SA, Alharbi SA. Influences of silicon carbide nanoparticles on graphite reinforced sisal (Agave sisalana) fiber hybrid composite: behaviour study. *Journal of Mechanical Science and Technology.* 2024;38: 2447–2453.
9. Venkatesh R, Dillikannan D, Ilavarasan N, Kamatchi RM, Das AD, Ammaiappan M, Arunkumar G, Kaliyaperumal G. An approach of nano-SiC-filled epoxy nanocomposite tensile and flexural strength enriched by the addition of sisal fiber. To be published in *Journal of The Institution of Engineers (India): Series D.* [Preprint] 2024. Available from: doi.org/10.1007/s40033-024-00680-1.
10. Mat Yazik MH, Hameed Sultan MT, Jawaid M, Mazlan N, Abu Talib AR, Md Shah AU, Safri SNA. Shape memory properties of epoxy with hybrid multi-walled carbon nanotube and montmorillonite nanoclay nanofiller. *Polymer Bulletin.* 2024;81: 951–968.
11. Liu Y, Zhang H, Yi C, Quan K, Lin B. Chemical composition, structure, physicochemical and functional properties of rice bran dietary fiber modified by cellulase treatment. *Food Chemistry.* 2021;342: 128352.
12. Arabani M, Shalchian MM, Rahimabadi MM. The influence of rice fiber and nanoclay on mechanical properties and mechanisms of clayey soil stabilization. *Construction and Building Materials.* 2023;407: 133542.

13. Puttaswamygowda PH, Sharma S, Ullal AK, Shettar M. Synergistic enhancement of the mechanical properties of epoxy-based coir fiber composites through alkaline treatment and nanoclay reinforcement. *Journal of Composites Science.* 2024;8(2): 66.
14. Mahuof AA, Alden AYQ, Faris AH, Al-hadithi MB, Al-Kubaisi O, Mahmood MH. The effect of a novel BYK dispersant for MWCNT on flexural properties of epoxy nanocomposites and hybrid carbon fiber composites. *Results in Engineering.* 2023;19: 101386.
15. Siva R, Nemali SSR, Gokul K, Kumar TA, Kunchapu SK. Comparison of mechanical properties and water absorption test on injection molding and extrusion-injection molding thermoplastic hemp fiber composite. *Materials Today: Proceedings.* 2021;47(14): 4382–4386.
16. Natrayan L, Surakasi R, Patil PP, Kaliappan S, Selvam V, Murugan P. Optimizing numerous influencing parameters of nano-SiO_2/banana fiber-reinforced hybrid composites using Taguchi and ANN approach. *Journal of Nanomaterials.* 2023;2023: 3317584.
17. Alsubari S, Zuhri MYM, Sapuan SM, Ishak MR, Ilyas RA, Asyraf MRM. Potential of natural fiber reinforced polymer composites in sandwich structures: a review on its mechanical properties. *Polymers.* 2021;13(3): 423.
18. Somvanshi KS, Gope PC. Effect of ultrasonication and fiber treatment on mechanical and thermal properties of polyvinyl alcohol/cellulose fiber nano-biocomposite film. *Polymer Composites.* 2021;42(10): 5310–5322.
19. Megahed M, Agwa MA, Megahed AA. Effect of ultrasonic parameters on the mechanical properties of glass fiber reinforced polyester filled with nano-clay. *Journal of Industrial Textiles.* 2022;51(2_suppl): 152808372091834
20. de Oliveira MM, Forsberg S, Selegård L, Carastan DJ. The influence of sonication processing conditions on electrical and mechanical properties of single and hybrid epoxy nanocomposites filled with carbon nanoparticles. *Polymers.* 2021;13(23): 4128.
21. Jagadeesh P, Puttegowda M, Mavinkere Rangappa S, Siengchin S. A review on extraction, chemical treatment, characterization of natural fibers and its composites for potential applications. *Polymer Composites.* 2021;42(12): 6239–6264.
22. Aravindh M, Sathish S, Ranga Raj R, Karthick A, Mohanavel V, Patil PP, Muhibbullah M, Osman SM. A review on the effect of various chemical treatments on the mechanical properties of renewable fiber-reinforced composites. *Advances in Materials Science and Engineering.* 2022;2022: 2009691.
23. Vivekanandhan M, Senthilkumar N, Deepanraj B, Naik N. Assessment on electrical discharge machining of ultrasonication assisted stir-casted AA8081-B4C-Gr hybrid composites and prediction using Levenberg–Marquardt technique. *Journal of Materials Research and Technology.* 2025;37: 1987–2004.
24. Gupta MK, Ramesh M, Thomas S. Effect of hybridization on properties of natural and synthetic fiber-reinforced polymer composites (2001–2020): a review. *Polymer Composites.* 2021;42(10): 4981–5010.
25. Zhang G, Zhang Y, Hou C, Zhang Q, Li Y, Jin Z, Li K, Wang H. High-temperature resistant, low dielectric SiO_2@Quartz fiber composites for high fidelity communication cables. *Ceramics International.* 2024;50(13): 23800–23807.
26. Kumar KR, Mohanavel V, Kiran K. Mechanical properties and characterization of polylactic acid/carbon fiber composite fabricated by fused deposition modeling. *Journal of Materials Engineering and Performance.* 2022;31: 4877–4886.
27. Wu Y, Wang Z, Xu L, Wang H, Peng S, Zheng L, Yang Z, Wu L, Miao JT. Preparation of silver-plated carbon nanotubes/carbon fiber hybrid fibers by combining freeze-drying deposition with a sizing process to enhance the mechanical properties of carbon fiber composites. *Composites Part A: Applied Science and Manufacturing.* 2021;146: 106421.
28. Mohammed M, Jawad AJAM, Mohammed AM, Oleiwi JK, Adam T, Osman AF, Dahham OS, Betar BO, Gopinath SCB, Jaafar M. Challenges and advancement in water absorption of natural fiber-reinforced polymer composites. *Polymer Testing.* 2023;124: 108083.
29. Al-Furjan MSH, Shan L, Shen X, Zarei MS, Hajmohammad MH, Kolahchi R. A review on fabrication techniques and tensile properties of glass, carbon, and Kevlar fiber reinforced polymer composites. *Journal of Materials Research and Technology.* 2022;19: 2930–2959.
30. Miniappan PK, Marimuthu S, Kumar SD, Gokilakrishnan G, Sharma S, Li C, Dwivedi SP, Abbas M. Mechanical, fracture-deformation, and tribology behavior of fillers-reinforced sisal fiber composites for lightweight automotive applications. *Reviews on Advanced Materials Science.* 2023;62(1): 20230342.
31. Sehar B, Waris A, Gilani SO, Ansari U, Mushtaq S, Khan NB, Jameel M, Khan MI, Bafakeeh OT, Tag-ElDin ESM. The impact of laminations on the mechanical strength of carbon-fiber composites for prosthetic foot fabrication. *Crystals.* 2022;12(10): 1429.
32. Parmiggiani A, Prato M, Pizzorni M. Effect of the fiber orientation on the tensile and flexural behavior of continuous carbon fiber composites made via fused filament fabrication. *The International Journal of Advanced Manufacturing Technology.* 2021;114: 2085–2101.

33. Nakagawa T, Ko S, Avery WB, Yang J, Salviato M. Computational and experimental investigation into the effects of platelet size and flow on the tensile properties of discontinuous fiber composites. *Composites Part A: Applied Science and Manufacturing.* 2025;199: 109170.
34. Fidan M, Yağci Ö. Effect of aging and fiber-reinforcement on color stability, translucency, and microhardness of single-shade resin composites versus multi-shade resin composite. *Journal of Esthetic and Restorative Dentistry.* 2024;36(4): 632–642.
35. Fráter M, Grosz J, Jakab A, Braunitzer G, Tarjányi T, Gulyás G, Bali K, Villa-Machado PA, Garoushi S, Forster A. Evaluation of microhardness of short fiber-reinforced composites inside the root canal after different light curing methods – An in vitro study. *Journal of the Mechanical Behavior of Biomedical Materials.* 2024;150: 106324.
36. Ning N, Wang M, Zhou G, Qiu Y, Wei Y. Effect of polymer nanoparticle morphology on fracture toughness enhancement of carbon fiber reinforced epoxy composites. *Composites Part B: Engineering.* 2022;234: 109749.
37. Mani M. Silica nanoparticle-enhanced mechanical properties and energy absorption behavior of hybrid fiber-reinforced polymer composites for structural applications. *Next Materials.* 2025;9: 101213.
38. Sekar S, Suresh Kumar S, Vigneshwaran S, Velmurugan G. Evaluation of mechanical and water absorption behavior of natural fiber-reinforced hybrid biocomposites. *Journal of Natural Fibers.* 2022;19(5): 1772–1782.
39. Ferede E, Atalie D. Mechanical and water absorption characteristics of sisal fiber reinforced polypropylene composite. *Journal of Natural Fibers.* 2022;19(16): 14825–14838.
40. Kumar S, Prasad L, Bijlwan PP, Yadav A. Thermogravimetric analysis of lignocellulosic leaf-based fiber-reinforced thermosets polymer composites: an overview. *Biomass Conversion and Biorefinery.* 2024;14: 12673–12698.
41. Giżyński M, Romelczyk-Baishya B. Investigation of carbon fiber–reinforced thermoplastic polymers using thermogravimetric analysis. *Journal of Thermoplastic Composite Materials.* 2021;34(1): 126–140.